Proceedings of 20th International Congress on Acoustics, ICA 2010

23-27 August 2010, Sydney, Australia

The radiation modes problem: exact solutions for the active control of sound power and the reconstruction of acoustic sources

Maury Cédric

SACADS Research Group, Laboratory of Mechanics and Acoustics (UPR CNRS 7051), Marseille, France

PACS: 43.40.Rj, 43.50.Sk, 43.50.Ki

ABSTRACT

The acoustic radiation modes, introduced 20 years ago by Borgiotti and mostly used in Active Structural Acoustic Control (ASAC), are a set of velocity distributions that independently contribute to the sound power radiated by a vibrating structure. A key feature is that the radiated sound power is reduced if the contribution of one of the radiation modes is cancelled. Moreover the radiation modes best capture the radiated sound power among all admissible velocity patterns. Hence, controlling the first radiation modes of a vibrating panel is an efficient ASAC strategy, despite the fact they are frequency-dependent and so, more difficult to sense/excite than the structural modes. Exact solutions have been found to the radiation modes problem for baffled planar structures. They are sought as velocity distributions with finite spatial support which have maximal energy concentration in a given radiation bandwidth. They satisfy a concentration problem the solutions of which involve prolate spheroidal wave functions which only depend on the structure geometry, on the frequency and on the physical properties of the surrounding fluid. An excellent agreement has been found between the closed-form radiation mode solutions and those calculated from an eigen-decomposition of the radiation resistance matrix. These analytical solutions have been generalized to determine closed-form expressions for the singular value decomposition of integral operators that govern the radiation of baffled planar structures into the far-field or the geometric near-field. These solutions provide further insight into the singular pressure and velocity vectors of the radiation problem. In particular, they provide an indication on the number of degrees of freedom of the radiated field detected above the noise threshold. This corresponds to the number of singular values, that should be accounted for, in the inverse source problem of reconstructing a stable approximation to an unknown boundary velocity from measurement of the radiated pressure field.

INTRODUCTION

An important problem arises in acoustics, namely the formulation of the total acoustic power radiated by a planar structure in terms of its radiation modes [1-4]. They correspond to a set of independent optimal velocity distributions defined on the surface of the structure, that best capture the sound power radiated among all possible velocity patterns [1]. As a consequence, we are certain to achieve optimal reduction of the sound power radiated by a vibrating structure if we cancel the contribution of any of its first radiation modes, which is not guaranteed when actively controlling the first normal modes of the structure due to high-order spillover effects [3]. The flip side of the coin is that the radiation mode shapes are frequency-dependent and they may be difficult to sense and/or excite in order to achieve active broadband noise reductions. However, it will be seen that the volumetric response of a baffled planar radiator, which is readily measured, is already a good approximation to the first radiation mode contribution at low frequencies.

As pointed out by Borgiotti [1], another key property of the radiation modes efficiencies is their plateau-like distribution, so that the sound power radiated by a structure can be expanded as a finite series of its radiation modes contributions, the number of which corresponds to the number of degrees of freedom (d.o.f.) of the radiated field. This is consistent with the well-known property, that the radiation operator acts as a low-pass spatial filter. Also it implies that, when implementing ASAC strategies, an accurate estimate of the radiated sound power to be minimized is obtained from a limited number of structural measurements that assess the first radiation modes contributions to the sound power.

BACKGROUND

The spherical radiator

Closed-form expressions are readily found for the radiation modes of a spherical shell of radius R that radiates into the whole fluid domain. They correspond to the spherical harmonic functions of degree n and order $|m| \le n$ depicted in Figure 1 and given by

$$v_{m,n}(\theta,\varphi) = P_n^{|m|}(\cos\theta)\,\mathrm{e}^{\mathrm{i}m\varphi}, \qquad [1]$$

with the corresponding squared radiation efficiencies

$$\sigma_{m,n}^2 = \frac{2\pi\rho c}{\left(k_0 R\right)^2 \left|\partial\left(h_n^{(2)}\left(k_0 R\right)\right)/\partial\left(k_0 R\right)\right|^2}, \quad [2]$$

with $k_0 R$ the dimensionless frequency and $h_n^{(2)}$ the spherical Hankel function of order n and of the second kind [5]. One retrieves from [2] the plateau-like distribution of the radiation modes efficiencies since $\sigma_{m,n}^2$ becomes negligible if $n > k_0 R$, so that the number of d.o.f. for the acoustic field radiated by a sphere scales on the number of acoustic wavelength spanned by the sphere radius. It can be shown that the spherical harmonics whose order is lower than $k_0 R$ are associated to radial travelling waves that contribute to the radiated sound power whereas those whose order is greater than $k_0 R$ are radial evanescent waves that only account for the reactive part of the radiated field.

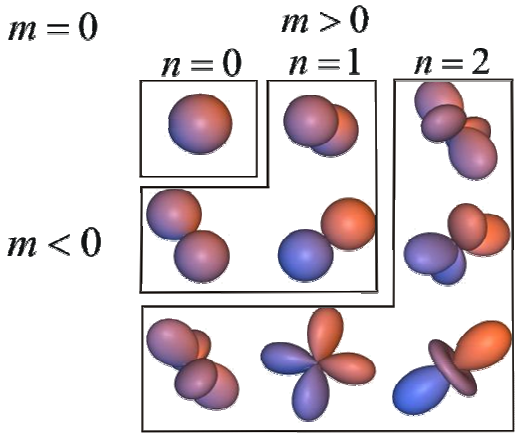

Figure 1. The first radiation modes of a full spherical radiator which are spherical harmonic functions.

General radiator

Apart from spherical and baffled planar radiators (as shown in this paper), exact expressions have not been found, to the best of our knowledge, for other types of radiators. One should then rely on their numerical computation. If one notes R_ω the integral far-field radiation operator, the acoustic pressure field p radiated by the boundary velocity v can be expressed as $p = R_\omega v$. The radiation modes can be computed from the Singular Value Decompositon (SVD) of the full radiation operator R_ω (that encompass all the supersonic radiating components) so that $R_\omega = \sum_n \sigma_n u_n v_n^*$. The radiation modes correspond to the right singular velocity distributions v_n such that [2]

$$R_\omega v_n = \sigma_n u_n . \quad [3]$$

Alternatively, if one left-iterates [3] with the adjoint R_ω^* of R_ω, the radiation modes v_n are obtained as the eigenmodes of the radiation resistance matrix $R_\omega^* R_\omega$ such that [6]

$$R_\omega^* R_\omega v_n = \sigma_n^2 v_n . \quad [4]$$

THE RADIATION MODES OF BAFFLED PLANAR STRUCTURES

Methodology

Closed-form expressions have been obtained for the radiation modes of baffled planar structures [7], which represent a generic class of radiators, often encountered in industrial or academic sound transmission and radiation problems. The radiation modes are velocity distributions with finite spatial support that concentrate most of the acoustic energy in the supersonic radiation bandwidth (delimited by the acoustic wavenumber k_0). In the two-dimensional case, one then has to find which velocity distributions $v(x)$, defined on a baffled beam of length $2L$, have maximal energy concentration, $\rho(k_0)$, in the radiation bandwidth, with

$$\rho(k_0) = \frac{\int_{|k|\le k_0} |V(k)|^2 dk}{\int_{\pm\infty} |V(k)|^2 dk} = \frac{\int_{-L}^{L}\int_{-L}^{L} v(x)\frac{\sin\left(k_0(x-x')\right)}{\pi(x-x')} v^*(x') dx\, dx'}{\int_{-L}^{L} |v(x)|^2 dx}, \quad [5]$$

in terms of $V(k) = \int_{-L}^{L} v(x) e^{ikx} dx$, the finite spatial Fourier transform of $v(x)$. This is achieved if $v(x)$ satisfies the following homogeneous Fredholm integral equation of the second kind with a sinc-like symmetric, positive definite kernel:

$$\int_{-L}^{L} v(x')\frac{\sin\left(k_0(x-x')\right)}{\pi(x-x')} dx' = \rho(k_0) v(x), \quad |x| \le L . \quad [6]$$

The kernel properties ensure the existence of a countable infinite sequence of non degenerate positive eigenvalues $\lambda_n(\alpha)$ and real eigenfunctions $\psi_n(\alpha, s)$ complete in both $L^2(-1,1)$ and $L^2(-\infty,\infty)$, for the integral equation [6] put in the following non dimensional form

$$\int_{-1}^{1} \frac{\sin\left(\alpha\left(s-s'\right)\right)}{\pi\left(s-s'\right)} \psi_n\left(\alpha,s'\right)ds' = \lambda_n\left(\alpha\right)\psi_n\left(\alpha,s\right),\ |s| \le 1 \text{ ,[7]}$$

with $\alpha = k_0 L$. As already observed in the context of Communication Theory [8], the integral operator [7] commutes with a much simpler second-order differential operator, the eigenfunctions of which are Prolate Spheroidal Wave Functions (PSWFs), so that both operators share the same spectral properties, which solve the acoustical concentration problem [6]. Hence, the integral equation [7] is explicitly solved by the following set of eigenvalues and eigenfunctions

$$\lambda_n\left(\alpha\right) = \frac{2\alpha}{\pi} R_{0n}\left(\alpha,1\right)^2 \quad \text{and} \quad \psi_n\left(\alpha,s\right) = S_{0n}\left(\alpha,s\right), \text{ [8]}$$

with $R_{0n}\left(\alpha,s\right)$ known as the radial PSWF, proportional to $S_{0n}\left(\alpha,s\right)$, the angular PSWF.

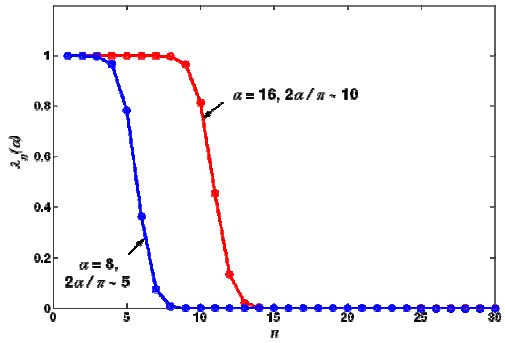

Figure 2. Plateau-like distribution of the first eigenvalues $\lambda_n\left(\alpha\right)$ for $n = 1,\cdots,30$, for $\alpha = 8$ (blue) and $\alpha = 16$ (red).

The eigenvalues $\lambda_n\left(\alpha\right)$ represent the concentration of energy contained by the eigenfunctions $\psi_n\left(\alpha,s\right)$ within $\left(-1,1\right)$. As shown on Figures 2 and 3, the fraction of energy of these functions within $\left(-1,1\right)$ increases when the dimensionless frequency parameter $\alpha = k_0 L$ increases. Moreover, the plateau-like distribution of the eigenvalues, already observed in [1], is now mathematically justified through the PSWFs properties, as shown in Figure 2. Indeed, for any given α, the radial PSWFs exponentially decay for $n \ge 2\alpha/\pi = 2k_0 L/\pi$, which provides a criterion on the number of d.o.f. of the radiated field or equivalently, on the number of radiation modes that mostly contribute to the sound power radiated (which scales linearly with frequency for the beam case).

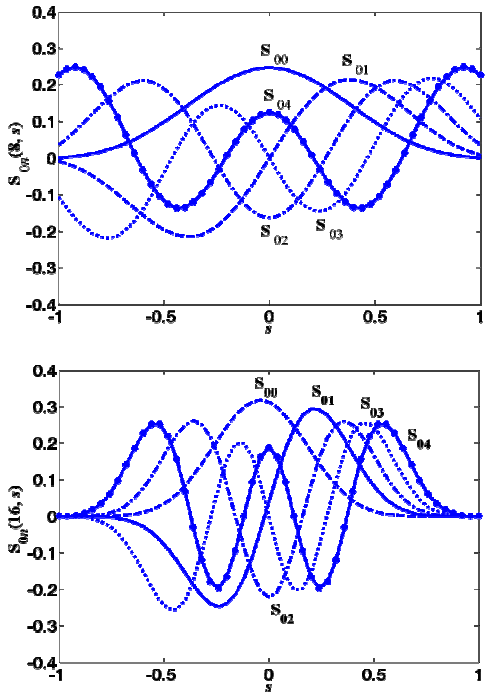

Figure 3. Prolate spheroidal wave functions $S_{0n}\left(\alpha,s\right)$, for $n = 0,\cdots,4$, and for $\alpha = 8$ (top) and $\alpha = 16$ (bottom).

Radiation modes of a baffled beam

If one considers the baffled beam of length $2L$ and width w depicted in Figure 4, Equations [8] provide closed-form expressions for the radiation mode shapes and efficiencies of the beam

$$\psi_n\left(k_0,x\right) = S_{0n}\left(k_0 L, \frac{x}{L}\right), \text{ [9]}$$

$$\sigma_n^2\left(k_0\right) = \frac{\left(k_0 w\right)\left(k_0 L\right)}{\pi} R_{0n}\left(k_0 L,1\right)^2, \text{ [10]}$$

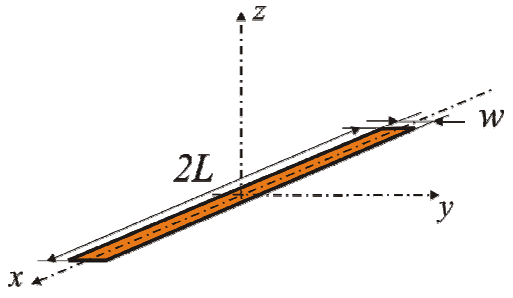

Figure 4. The baffled beam geometry.

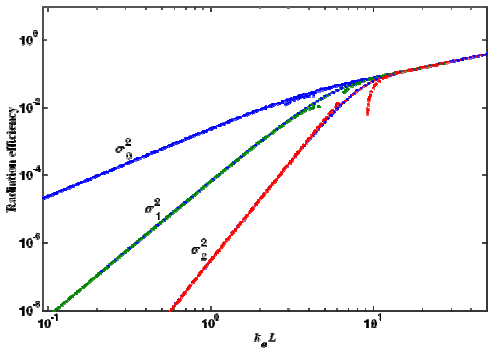

Figure 5. Analytical approximations (dashed) and numerical calculation (bold) of the first three radiation modes efficiencies of a baffled beam together with the low- and high-frequency asymptotics (dash-dotted).

The first three exact radiation mode efficiencies are calculated from Eq. [10] and plotted in Figure 5 for a beam ratio $w/L = 1/64$, together with low- and high-frequency asymptotic developments, also obtained from Eq. [10]. Their values coincide with those computed using Eq. [4] from an eigendecomposition of the beam radiation resistance matrix. The largest eigenvalue, σ_0, can be interpreted as the largest fraction of acoustic energy radiated by a velocity distribution ψ_0 on the beam among all admissible velocity distributions. Furthermore, σ_1 can be interpreted as the largest fraction of acoustic energy radiated among all velocity distributions orthogonal to ψ_0. More generally, the mode ψ_n corresponds to the optimal surface velocity distribution with maximum radiation efficiency, σ_n, among all velocity distributions orthogonals to $\psi_0, \psi_1, \cdots, \psi_{n-1}$.

Radiation modes of a baffled panel

The closed-form solutions [9-10] for the radiation modes of a baffled beam have been extended to the three-dimensional case of a baffled panel, assuming that the sinc-like kernel of the radiation operator can be put in a separable form along each of the panel directions, which is an accurate approximation at low frequencies, i.e. for $k_0 L_x \leq \pi$, with L_x the panel length. Analytical approximations to the radiation mode shapes and efficiencies of a baffled panel can thus be obtained as follows

$$\psi_{m,n}(k_0, x, y) = S_{0m}\left(k_0 L_x, \frac{x}{L_x}\right) S_{0n}\left(k_0 L_y, \frac{y}{L_y}\right), \quad [11]$$

$$\sigma^2_{m,n}(k_0) = \frac{(k_0 L_x)(k_0 L_y)}{\pi^2} R_{0m}(k_0 L_x, 1)^2 R_{0n}(k_0 L_y, 1)^2, \quad [12]$$

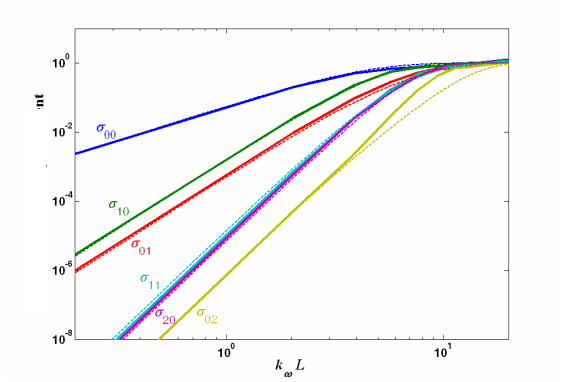

Figure 6. Analytical approximations (dashed) and numerical calculation (bold) of the first six radiation modes efficiencies of a baffled panel.

As shown on Figures 6 to 8, the analytical expressions [11-12] still provide reasonable approximations to the panel radiation modes shapes and efficiencies up to $k_0 L_x \leq 7$. In particular, low-frequency asymptotics of [12] provide an explanation of the grouping properties of the radiation modes efficiencies, already observed in [9], and given by a $(n+m)$ power law of the dimensionless frequency $k_0 L_x$. It can be seen from Figure 7 that the net volume velocity of the panel well approximates the piston-like shape of the first radiation mode, which is useful for low-frequency ASAC applications. It becomes a dome-shaped mode at higher frequencies, difficult to sense/excite, although it can be estimated from velocity measurements passed through suitable frequency-dependent radiation filters that implement Eqs. [11-12].

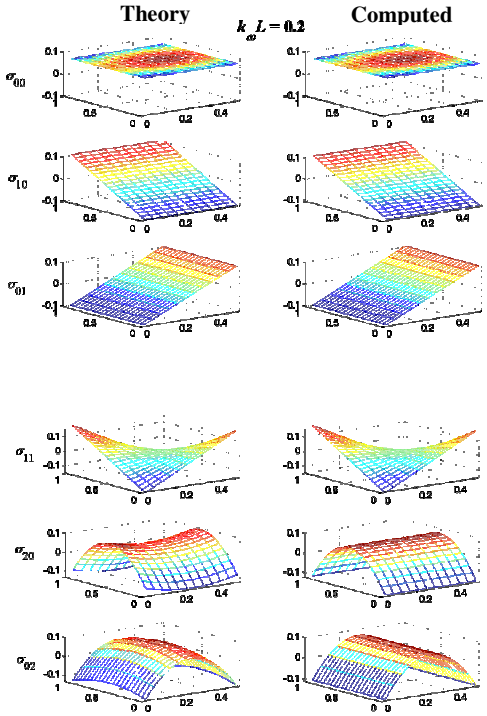

Figure 7. The low-frequency modes shapes of the first six radiation modes of a baffled panel (left column: analytical approximations ; right column: numerical calculations).

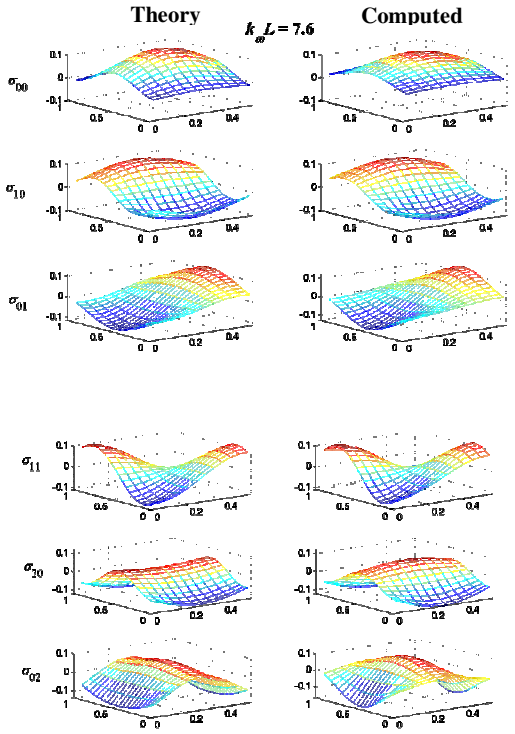

Figure 8. The mid-frequency modes shapes of the first six radiation modes of a baffled panel (left column: analytical approximations ; right column: numerical calculations).

EXACT SOLUTIONS TO THE INVERSE SOURCE PROBLEM

Exact SVD of the radiation operators

Closed-form expressions for the radiations modes [9-12] have been generalized to obtain exact expressions for the singular system of the far-field and geometric near-field radiation operators, as detailled in [10]. The far-field (resp. geometric near-field) radiated pressure distributions are spatial Fourier (resp. Fresnel) transforms of the boundary velocity, with compact integral operators. An exact SVD of the integral operators is thus obtained from the invariance properties of the PSWFs with respect to the complex exponential radiation kernels, that generalize the invariance property [7-8] associated to the sinc-like kernel.

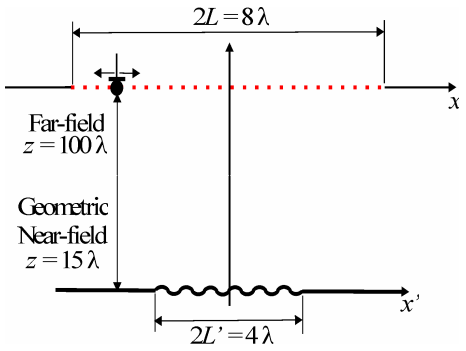

Figure 9. The vibrating beam and the far-field (resp. geometric near-field) observation line.

Assuming an array of microphones of length $2L$ linearly distributed in the geometric near-field of a baffled beam of length $2L'$, as depicted in Figure 9, the singular velocity and radiation patterns, v_n and u_n, and the corresponding singular values σ_n, all related by [3], are given by

$$u_n\left(\gamma_R, x\right) = \mathrm{i}^{n+1/2}\mathrm{e}^{-\mathrm{i}kz}\mathrm{e}^{-\mathrm{i}\frac{\pi x^2}{\lambda z}} S_{0n}\left(\gamma_R, \frac{x}{L}\right), \quad [13]$$

$$\sigma_n\left(\gamma_R\right) = \frac{2\rho c}{\sqrt{\lambda z}} R_{0n}\left(\gamma_R, 1\right), \quad [14]$$

$$v_n\left(\gamma_R, x'\right) = \mathrm{e}^{\mathrm{i}\frac{\pi x'^2}{\lambda z}} S_{0n}\left(\gamma_R, \frac{x'}{L'}\right), \quad [15]$$

with $\gamma_R = k_0 L'\left(L/z\right)$ the space-bandwidth parameter. Figure 10 shows that the first singular velocity and radiation patterns of a baffled beam computed at $z = 15\lambda$ from the radiator with a SVD toolbox agree well (in real parts, but also in imaginary parts, not shown) with the exact values given by Eqs. [13, 15].

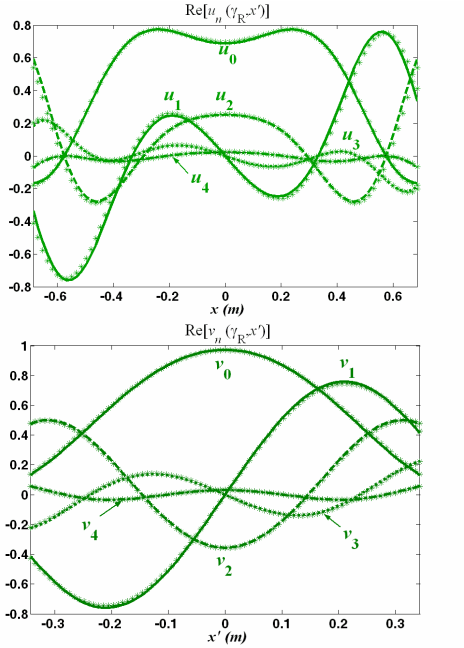

Figure 10. Exact (bold) and SVD computed (asterisks) real part of the first normalised singular radiation (top) and velocity (bottom) patterns for a geometric near-field observation line.

An excellent correlation is also noted in Figure 12 for the singular system of the full far-field radiation operator, given by

$$u_n\left(\gamma_H, \theta\right) = \mathrm{i}^{n+1/2}\mathrm{e}^{-\mathrm{i}kR} S_{0n}\left(\gamma_H, \sin\theta\right), \quad [16]$$

$$\sigma_n\left(\gamma_H\right) = \frac{2\rho c}{\sqrt{\lambda R}} R_{0n}\left(\gamma_H, 1\right), \quad [17]$$

$$v_n\left(\gamma_H, x'\right) = S_{0n}\left(\gamma_H, \frac{x'}{L'}\right), \quad [18]$$

with $\gamma_H = k_0 L'$. They are associated to acoustic radiation of the beam onto the hemi-circular observation domain depicted in Figure 11. It is shown in Figure 12 that each supersonic radiation pattern beams in a particular direction within each quadrant, with the least radiating modes beaming towards grazing angles from the source distribution. This feature was initially observed by Photiadis [2].

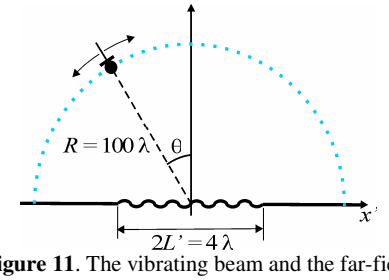

Figure 11. The vibrating beam and the far-field observation arc

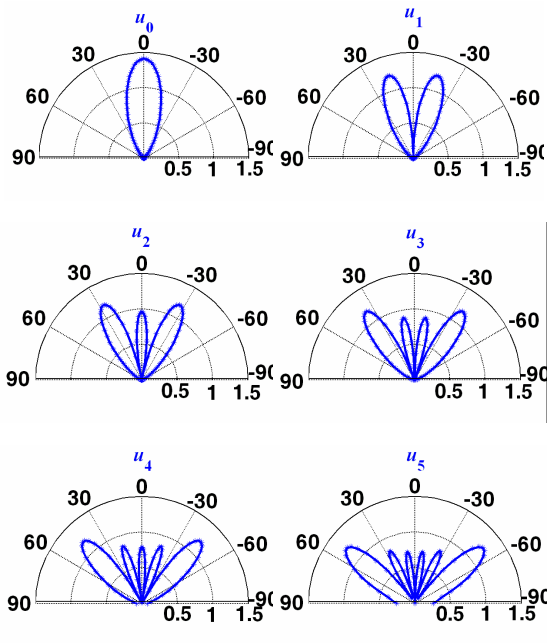

Figure 12. Exact (bold) and SVD computed (asterisks) directivity diagrams of the first normalised singular radiation patterns for a hemi-circular far-field observation domain.

Figure 13 shows the exponential decay (on a logarithmic scale) of the first singular values associated with the far-field (rectilinear and hemi-circular) and geometric near-field (rectilinear) radiation operators and determined from the analytic expressions [14, 17]. Their values coincide with those computed from an SVD of the acoustic transfer matrix that relates the amplitudes of the radiated pressures obtained at 81 observation points evenly spaced over the observation array to the strengths of 81 monopoles uniformly distributed over the beam length.

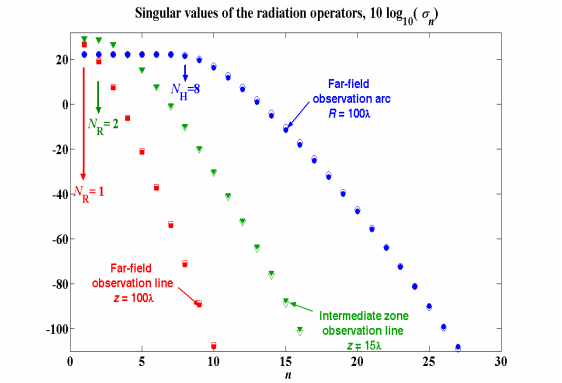

Figure 13. The first singular values of the radiation operators (exact: open ; computed: filled) and the number of d.o.f. of the radiated field.

The influence of the height of the observation line above the elastic beam results in a greater angular space-bandwidth parameter γ_R in the geometric near-field (or intermediate) case with respect to the far-field case. This parameter scales on the angular aperture of the observation domain and on the dimensionless frequency. As illustrated in Figure 13, a greater number of singular radiation (respectively velocity) functions efficiently contribute to the representation of the acoustic pressure (respectively boundary velocity) field in the intermediate case with respect to the far-field case. However, the greatest number of d.o.f. is captured assuming a far-field hemi-circular observation domain that encompass all the supersonic radiating components.

Insights into the inverse source problem

Referring to Figures 9 or 11, the acoustic source reconstruction problem aims at retrieving an approximation of the unknown boundary velocity v from measurements of the radiated pressure field, $\tilde{p} = R_{\omega} v + \tilde{n}$, in the observation domains, where $\tilde{n}$ is a white additive noise. A model-based approach requires an inversion of the radiation filter, readily obtained in terms of the singular system of the radiation operator (see Refs. [11,12]), and which is expressed as a series of the singular velocity modes weighted by the inverse of the singular values, σ_n^{-1}. Due to their plateau-like distribution shown in Figure 13, a stable regularised approximation to the reconstructed velocity, $\tilde{v}_{\alpha}$, is only obtained after low-pass filtering the smallest singular values that would otherwise contribute to amplify the perturbation error (see Ref. [10]). A low-pass filtered approximation to the retrieved velocity reads:

$$\tilde{v}_{\alpha} = \sum_{n=0}^{\infty} f_{\alpha}\left(\sigma_n\right) \frac{\left\langle \tilde{p}, u_n \right\rangle_{\Omega}}{\sigma_n} v_n, \quad [19]$$

in terms of $\langle g, h \rangle_{\Omega}$ the scalar product defined on the observation domain Ω and $f_{\alpha}(\sigma)$ a low-pass filter with regularisation parameter α carefully chosen to balance the regularisation and perturbation errors. Typically, the L-curve technique or the Generalized Cross-Validation method have

proved to be useful to determine α without prior knowledge of the noise variance.

Due to the exponential decay of the singular values associated to the far-field or geometric near-field radiation operators, a singular value discarding method appears to be a suitable candidate to provide a stable solution. In this case, the low-pass filter is a rectangle window function and the regularisation parameter, $\alpha = N_{\text{eff.}}$, corresponds to the effective number of d.o.f. of the radiated field in presence of noise, so that $f_{\alpha}(\sigma_n) = \text{rect}_{N_{\text{eff.}}}\lfloor \sigma_n \rfloor$. $N_{\text{eff.}}$ scales on the dimensionless frequency and it is a function of the signal-to-noise ratio, δ/σ. It reads [10]:

$$N_{\text{eff.}} = \left\lfloor \frac{2k_0 L'}{\pi} \sqrt{1 + \frac{1}{(k_0 z)^2} W_0^2\left(k_0 z\right)\frac{\delta}{\sigma}} \right\rfloor, \qquad [20]$$

the integer part, $\lfloor\ \rfloor$, of an expression that involves the Lambert function, W_0. This number ensures a stable reconstruction of the boundary velocity with a spatial resolution $2L'/N_{\text{eff.}}$, assuming that the zeros of the PSWFs are evenly distributed, which is a reasonable assumption.

Figure 14 shows simulation results for the reconstruction of the piston-like motion of a beam with unit velocity amplitude, from far-field measurements of the acoustic pressure radiated by the beam over a rectilinear or hemi-circular observation domain. It can be seen that the spatial resolution increases with frequency or when the observation domain captures all of the supersonic radiating components, as it is the case for the observation arc with respect to the observation line which only detects a fraction of the radiated components. In both cases, the resolution increases as the effective number of d.o.f. of the radiated field increases.

Clearly, the presence of noise degrades the accuracy of the reconstruction, but not its resolution. This is due to the exponential decay of the singular values of the far-field radiation operator. This would not be the case when considering a (hydrodynamic) near-field radiation operator with a less steeper decay of the singular values and for which the amount of noise in the measured data degrades both the accuracy and the resolution of the reconstruction.

CONCLUSIONS

Based on the solution to a vibro-acoustic concentration problem, analytical expressions have been obtained for the SVD of the radiation operators that map the boundary velocity of a baffled structure onto the pressure distribution radiated over a number of observation domains in the far-field and geometric near-field regions. In particular, it is shown that the radiation modes of a baffled planar structure correspond to the singular velocity patterns of the operator governing the acoustic radiation over a far-field hemi-circular arc surrounding the structure. The closed-form expressions of the singular system are found to correlate well with the numerical solutions obtained from an SVD of associated radiation matrices.

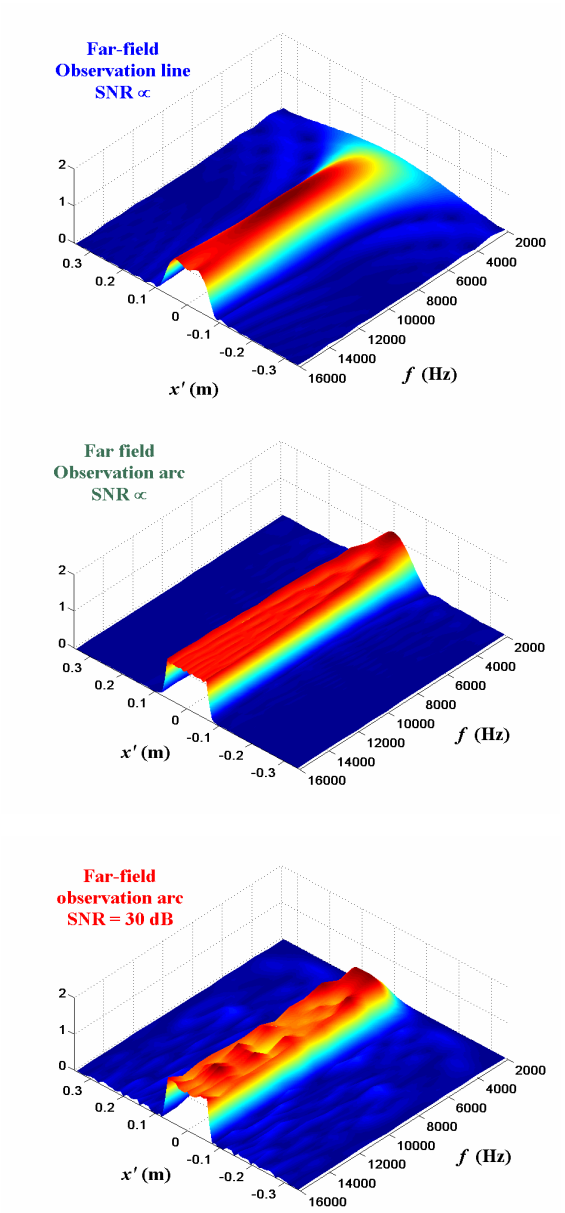

Figure 14. Piston-like boundary velocity reconstructed from far-field pressure data vs. frequency

Stable estimates of the reconstructed boundary velocity in the presence of noise have been obtained with singular value discarding regularization, with an exact expression of the cut-off wavenumber for the corresponding filter factor in terms of the regularization parameter. Exact expressions for the cut-off wavenumber have also been formulated for other typical schemes such as Tikhonov low-pass filtering and Landweber iterations [10].

The regularization scheme based on the truncated SVD is well suited for source reconstruction from far-field or intermediate regions, and a stable solution is found by decomposing the unknown boundary velocity into a finite number of efficiently radiating singular velocity patterns. They correspond to the effective number of d.o.f. of the radiated field for which exact expressions have been deduced from the singular system of the radiation operators in the far-field and intermediate regions. This number scales on the spatial frequency bandwidth of the radiated pressure field. Its inverse yields to an estimate of the spatial resolution limits

that can be achieved in the inverse source reconstruction problem for different configurations of the observation domains. In particular, the smallest resolution loss with respect to the Rayleigh resolution limit, π/k_0, is reached when one attempts to reconstruct the boundary velocity from pressure data acquired over a hemi-circular arc. This result is shown to be weakly influenced by the presence of spatially white noise in the far-field data.

One should note that the SVD-based approach provides an optimal basis (PSWFs for baffled planar structures radiating in the far-field or the geometric near-field) for decomposing the pressure and velocity distributions of a radiator, both defined over a finite spatial support. This is unlike Fourier-based NAH methods (Near-Field Acoustical Holography) which use a decomposition of the pressure and velocity distributions over a continuum of wavenumber components with complex exponential basis functions with spatially unbounded support. These functions would be optimal if the radiator and the observation domains were unbounded, which is not the case in practice. An interesting point is that Eqs. [13, 14] tend towards complex exponential functions when L and L' span several acoustic wavelengths, in which case the radiation operator becomes homogeneous and is, as expected, associated to Fourier basis functions.

ACKNOWLEDGMENTS

The author would like to thank Prof. S. J. Elliott (ISVR, United Kingdom) and Dr. T. Bravo Maria (CAEND, Spain) for their insightful contributions to this long-term research.

REFERENCES

1 G.V. Borgiotti, "The power radiated by a vibrating body in an acoustic fluid and its determination from boundary measurements" *J. Acoust. Soc. Am.* **88**, 1884–1893 (1990)
2 D.M. Photiadis, "The relationship of singular value decomposition to wave-vector filtering in sound radiation problems" *J. Acoust. Soc. Am.* **88**, 1152–1159 (1990)
3 S.J. Elliott and M.E. Johnson, "Radiation modes and the active control of sound power" *J. Acoust. Soc. Am.* **94**, 2194–2204 (1993)
4 K.A. Cunefare and M.N. Currey, "On the exterior acoustic radiation modes of structures" *J. Acoust. Soc. Am.* **96**, 2302–2312 (1994)
5 PH. M. Morse and H. Feshbach, *Methods of theoretical physics* (McGraw-Hill, New York, 1953)
6 A. Sarkissian, "Acoustic radiation from finite structures" *J. Acoust. Soc. Am.* **90**, 574–578 (1991)
7 C. Maury and S.J. Elliott, "Analytic solutions of the radiation modes problem and the active control of sound power" *Proc. Roy. Soc. A* **461**, 55–78 (2005)
8 D. Slepian and H.O. Pollack, "Prolate spheroidal wave functions, Fourier analysis and uncertainty. I.".*Bell Syst. Tech. J.* **40**, 43–64 (1961)
9 K.A. Cunefare, M.N. Currey, M.E. Johnson and S.J. Elliott, "The radiation efficiency grouping of the free-space acoustic radiation modes" *J. Acoust. Soc. Am.* **109**, 203–215 (2001)
10 C. Maury and T. Bravo, "Analytic solutions to the acoustic source reconstruction problem" *Proc. Roy. Soc. A* **464**, 1697–1718 (2008)
11 S.F. Wu, "Methods for reconstructing acoustic quantities based on acoustic pressure measurements" *J. Acoust. Soc. Am.* **124**, 2680–2697 (2008)
12 B-K. Kim and J-G. Ih, "On the reconstruction of the vibro-acoustic field over the surface enclosing an interior space using the boundary element method" *J. Acoust. Soc. Am.* **100**, 3003–3016 (1996)